academicJournals

Vol. 8(31), pp. 1570-1580, 23 August, 2013
DOI: 10.5897/IJPS2013.3974
ISSN 1992 - 1950 © 2013 Academic Journals
http://www.academicjournals.org/IJPS

International Journal of Physical Sciences

Full Length Research Paper

Optical properties of as-deposited TiO_2 thin films prepared by DC sputtering technique

M. M. Abd El-Raheem[1,2] and Ateyyah M. Al-Baradi[1]

[1]Department of Physics, Faculty of Science, Taif University, Taif 888, Saudi Arabia.
[2]Department of Physics, Faculty of Science, Sohag University, Sohag 82524, Egypt.

Accepted 8 August, 2013

Amorphous titanium dioxide TiO_2 thin films have been deposited using the dc sputtering technique. The structure of the films was analyzed by X-ray diffraction and the results showed non-crystalline behavior. The optical properties of these thin films have been investigated by means of optical reflectance and transmittance spectra. The optical energy gap E_g, the Urbach tails E_u, the single oscillator energy E_o, the dispersion energy E_d and the optical constants as refractive index n, extinction coefficient k dielectric constant and optical conductivity were estimated.

Key words: Titanium dioxide, optical energy gap, refractive index, oscillator energy, dispersion energy.

INTRODUCTION

Titanium dioxide TiO_2 thin films are the most widely used coatings due to their desirable properties, such as good adhesion, high stability against mechanical abrasion, chemical attach, and high temperature (Pulker, 1984; Ritter, 1975). Therefore, they are used as single-layer or multilayer optical coatings (Macleon, 1986). Titanium dioxide thin films have been largely studied as photo anodes in the process of photo electrolysis of water in solar energy conversion systems, electrochromic materials for display devices, smart windows, antireflective coatings, optical filters (Yoko, et al., 1988; Doeuff et al., 1986; Livage, 1986; Nabavi et al., 1989; Dislich and Hinz, 1982). Titanium dioxide films can be prepared using different kind of methods: thermal or anodic oxidation of titanium, electron beam evaporation, ion sputtering, chemical vapour deposition and sol-gel method (Yoldas, 1980; Henry, 1978; Lottiaux et al., 1989; Babuji et al., 1983; Yeung and Lam, 1983; Ozer et al., 1992; Yun et al., 2003). It was reported that titanium dioxide exists in three different phases: anatase, rutile, and brookite. Only anatase, rutile and amorphous film have been observed in TiO_2 thin films up to now (Lo¨ et al., 1994). TiO_2 film in anatase phase has a variety of application prospects in the field of environmental protection (Dumitriu, et al., 2000; Takeda et al., 2001). The rutile structure of TiO_2 thin film is known as a good blood compatibility material and can be used as artificial heart valves (Zhang et al., 1996). Much technique was used to achieve TiO_2 thin film (Takeda et al., 2001; Watanabe et al., 2000). Magnetron sputtering is one of the most easily to industrialize, and to achieve the high quality thin film in large area substrates (Dumitriu et al., 2000; Treichel and Kirchhoff, 2000). Mid-frequency ac magnetron sputtering using pure titanium target was

*Corresponding author. E-mail: elneh@yahoo.com.

PACS. 78.20.Ci optical constants.

studied widely (Bra¨uer et al., 1998; Hou et al., 2000). The optical constants of TiO_2 thin films were studied using spectroscopic ellipsometry.

The aim of the present work is to prepare thin films of TiO_2 using dc sputtering technique and to study their optical properties with change in their thicknesses.

EXPERIMENTAL TECHNIQUE

Titanium dioxide TiO_2 thin layers were prepared by DC sputtering under a base pressure (95% argon + 5% O_2) of 15 mTorr. TiO_2 target (from Cathey) with a purity of 99.998% and 3 inch diameter was used. The target-substrate distance was fixed at 11 cm. For obtaining homogeneous films, periodic motion of 2 rpm of the substrates was adopted. Thin films of TiO_2 were deposited on a pre-cleaned glass substrate using UNIVEX 350 sputtering unit with dc power model Turbo drive TD20 classic (Lybold) and rate thickness monitor model INFICON AOM-160. The structural characteristics of TiO_2 thin films were investigated by X-ray diffraction pattern. Philips X-ray diffractometer model X' Pert was used for the measurements which utilized monochromatic CuKα = 1.5406 Å radiation operated at 40 kV and 25 mA.

Reflectance R and transmittance T measurements under near-normal incidence in the spectral range 200-1000 nm were performed by using double beam spectrophotometer (JASCO model V-670 UV-VIS-NIR). The substrate temperature was kept at 25°C during deposition. In this paper, we report on the optical properties of amorphous TiO_2 thin films deposited by dc sputtering

Theory and calculations

For obtaining the optical energy gap E_{op}, the following equation was used (Pal et al., 1993):

$$(\alpha h\upsilon)^b = A(h\upsilon - E_{op}) \quad (1)$$

where the absorption coefficient α can be expressed as (Ali, 2005):

$$\alpha = \frac{1}{d} Ln\left(\frac{(1-R)^2}{T}\right) \quad (2)$$

The absolute value of transmittance T is given by (El-Nahass, 1992):

$$T = \left(\frac{I_{fr}}{I_g}\right)(1 - R_g) \quad (3)$$

$(h\nu)$ is the incident photon energy, R is the reflectance, R_g is the reflectance of glass substrate, I_{ft} is the intensity of light passing through the film-glass system, I_g is the intensity of the light passing through the reference glass and d is the film thickness. The absolute value of the reflectance R is given by (Bakry and El-Naggar, 2000):

$$R = [(\frac{I_{fr}}{I_m})R_m(1 + [1 - R_g]^2) - T^2 R_g \quad (4)$$

I_{fr} is the intensity of light reflected from the sample, I_m is the intensity of light reflected from the reference mirror.

The refractive index n was calculated from the following equation (El-Nahass et al., 2008):

$$n = \frac{1+R}{1-R} + [\frac{4R}{(R-1)^2} - k^2)]^{1/2} \quad (5)$$

where $k = \alpha\lambda / 4\pi$ is the absorption index, and λ the is incident wavelength.

The amount of tailing can be estimated to a first approximation by plotting the absorption edge data in terms of an equation originally given by Urbach (1953), which has been applied to many glassy materials. The exponential depends on the absorption coefficient, (α) and photon energy ($h\nu$). It has been found that $h\nu$ holds over several decades for a glassy material and takes the formula:

$$\alpha = \alpha_o e^{\frac{h\upsilon}{E_u}} \quad (6)$$

Using DiDomenico dispersion relationship (Wemple and DiDomenco, 1973), the single oscillator energy E_o and dispersion energy E_d can be calculated:

$$(n^2 - 1)^{-1} = \frac{E_o}{E_d} - \frac{1}{E_o E_d}(h\upsilon)^2 \quad (7)$$

For obtaining the lattice dielectric constant ε_L, the following equation is used (El-Nahass et al., 2010):

$$\varepsilon_1 = n^2 = \varepsilon_L - \frac{e^2 N}{4\pi\varepsilon_o m^* c^2}\lambda^2 \quad (8)$$

Where e is the elementary charge, ε_o is the permittivity of free space, N/m* is the ratio of free carrier concentration to the effective mass.

RESULTS AND DISCUSSION

Structural investigation

X-ray diffraction patterns of titanium dioxide TiO_2 thin films of as-prepared showed amorphous structure as shown in Figure 1 where the patterns did not include any peak representing crystallization.

Optical characterization

Effect of thickness of TiO_2 on the optical properties

Figure 2 depicts the changes of the transmittance T(%) with the incident wavelength. Throughout the range of the incident wavelength from 200 to 500 nm, there were peaks belonging to the films of thicknesses 100, 120, 150, 175 and 200 nm and had the values 60, 72, 83, 87, and 90% at 380, 380, 400, 405 and 425 nm, respectively. It can be noticed that the peaks of the transmittance were shifted toward a longer wavelength with increasing the thickness of the films as shown in Figure 2. The highest values of the transmittance were followed with decreasing their values with prolongating the wavelength for the considered thin films except for the film of thickness 100 nm. It can be noticed also that the

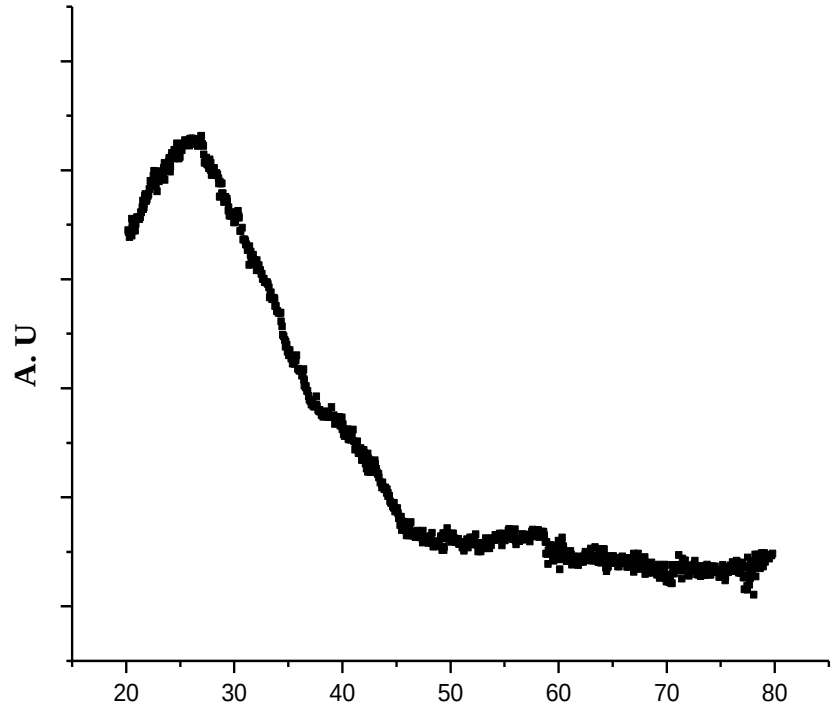

Figure 1. X-ray diffraction patterns of as0prepared $Ti0_2$ thin film.

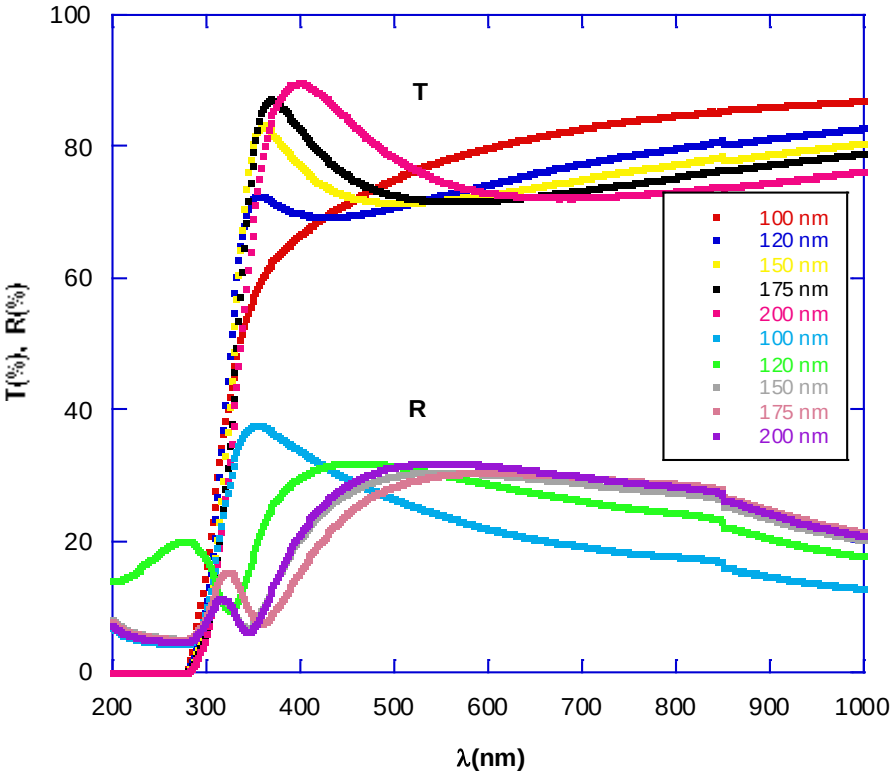

Figure 2. The optical transmittance T (λ) and reflectance R (λ) forthe as prepared TiO_2 thin films of different thicknesses.

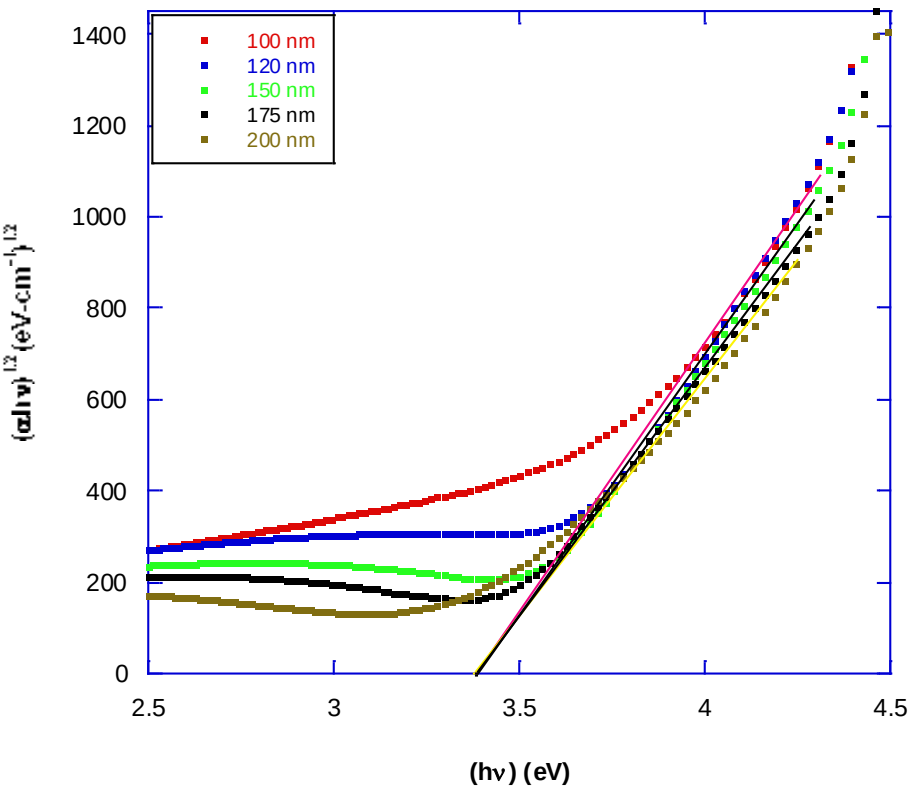

Figure 3. Plots of $(\alpha h\nu)^{1/2}$ vs. $h\nu$ for as-prepared TiO_2 thin films of different thicknesses.

transmittance decreases with increasing the film thickness which can be due to an increase in both reflection and absorption in the thin films (Al-Ofi et al., 2012). In addition, film structure may lose its homogeneity with increasing the film thickness due to accumulation of different types of structural faults, hence increasing film absorption. The transmittance loss at longer wavelengths results from photon-electron interaction, which can scatter the photons. This loss occurs from both reflection and absorption. Reflection in this range is not strictly a surface phenomenon (Robert et al., 2005). However, reflection from the bulk of the material can occur, provided that the photon escapes the surface. If the scattered photon does not escape the surface, it can be concluded to have been absorbed (Robert et al., 2005).

The results of reflectance verify the transmittance one as shown in Figure 2, where the reflectance increased in the region of decreasing the transmittance. On the other hand, the top of the transmittance were corresponding to the bottom of the transmittance. Figure 3 shows the relation $(\alpha h\upsilon)^{1/2}$ vs. $(h\upsilon)$ for as-prepared TiO_2 thin films with different thicknesses. The values of the allowed indirect optical energy gap E_{op} can be obtained from the plots of $(\alpha h\upsilon)^{1/2}$ versus $(h\upsilon)$ by extrapolating the linear portion of the plots of $(\alpha h\upsilon)^{1/2}$ versus $(h\upsilon)$ to $\alpha = 0.0$ as shown in Figure 3. The estimated values of the optical energy gap were found to be independent on the film thickness where it had the same value 3.36 eV for all the considered film thickness. This value 3.36 eV of the optical gap of the thin films under test is very close to the reported one 3.27 eV (Ya-Qi et al., 2003). The Urbach tails (width of the band tails of the localized states) represents the degree of disorder in an amorphous semiconductor E_u for as-prepared TiO_2 thin films can be obtained from the slopes of the straight lines of the plot Ln(α) versus $h\upsilon$ as shown in Figure 4. Results of Urbach tails confirmed the results of optical gap, where E_u was found to have the same value 0.37±eV within the experimental error for all the considered films (El-Raheem et al., 2012).

The variations of both the real part of the refractive index n and the extinction coefficient k with wavelength are shown in Figure 5. It is apparent that the refractive index decreases with increasing the incident wavelength in the visible range of frequency revealing the normal dispersion. Further, the refractive index increases with increasing the film thickness; this may be due to changing the film thickness which could change the density and/or the polarization of the material of the thin films. On the other hand, the variations of the extinction

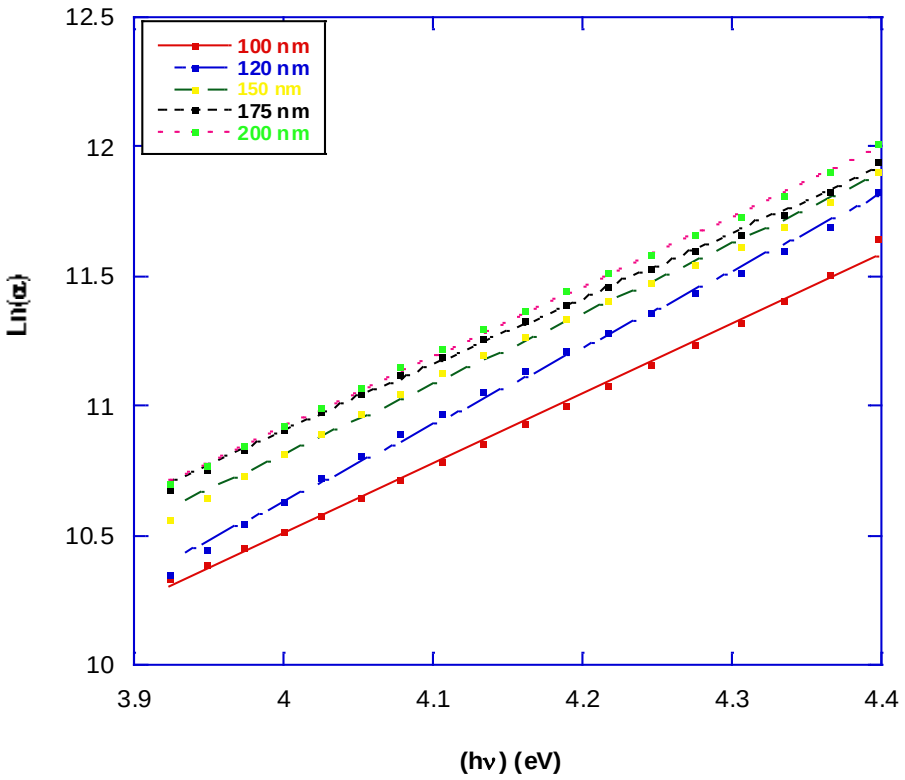

Figure 4. Plots of Ln(α) vs. photon energy for as-prepared TiO_2 thin films of different thicknesses.

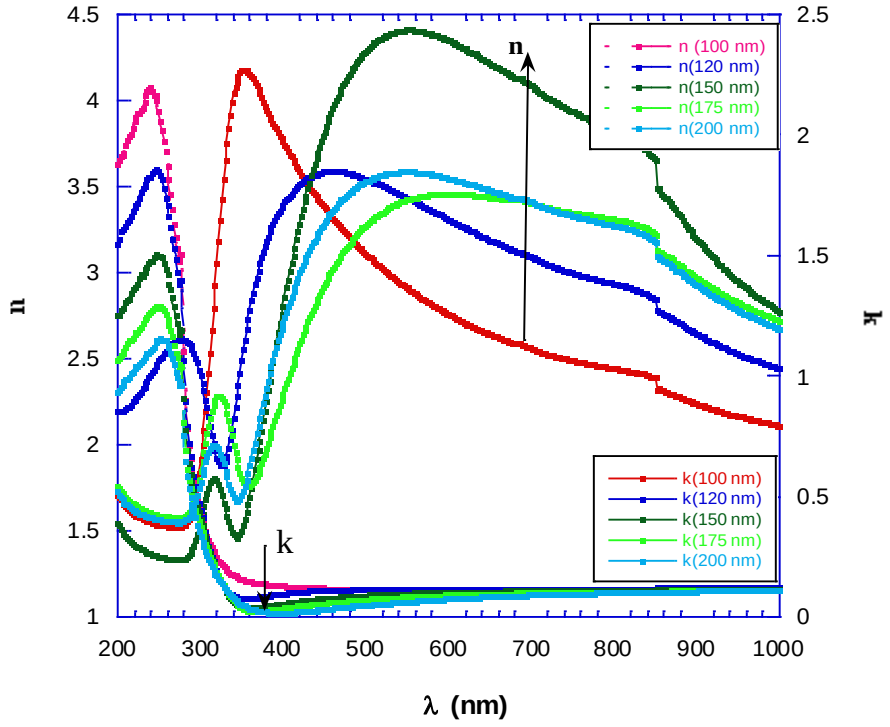

Figure 5. Spectra of the refractive index n and the extenction coefficiont k of TiO_2 thin films of different thicknesses.

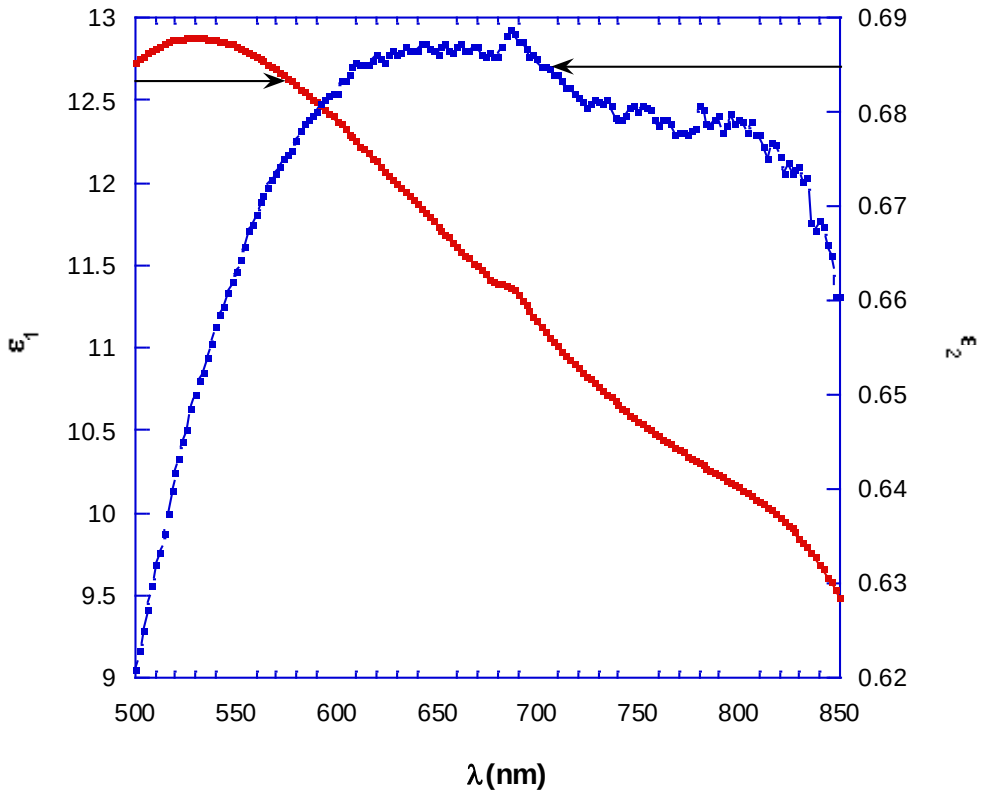

Figure 6. Variations of the average values of real and imaginary part of the dielectric function with incident wavelength.

coefficient k reverse the behavior of the refractive index. Figure 6 depicts the changes of both the average values (belonging to the different thicknesses of the thin films under test) real ε_1 and imaginary ε_2 parts of the dielectric function with incident wavelength. The real part of the dielectric constant relates to dispersion, whereas dissipative rate of the electromagnetic wave in the dielectric medium is provided by imaginary part. It is clear that the variations of ε_1 follows the same trend as the real part of the refractive index and the imaginary part ε_2 follows the behavior of the extinction coefficient k with the incident wavelength as shown in Figure 5. Figure 7 depicts the variations of the loss factor tan δ with wavelength indicating that the loss factor decreases sharply with increasing the wavelength within the range from 300 to 400 nm and the increases slightly. To calculate the real and imaginary components of optical conductivity the following equations are used (Caglar et al., 2007):

$$\sigma_1 = \omega\varepsilon_2\varepsilon_0 \text{ and } \sigma_2 = \omega\varepsilon_1\varepsilon_0$$

where ω is the angular frequency, ε_0 is the permittivity of free space. The spectra of real and imaginary parts of the optical conductivity are shown in Figure 8. It can be seen that both the real and imaginary part increases with increasing the photon energy up to 2.6 eV which can be attributed to excitation of electrons by photon energy (Caglar et al., 2007).

Real part of optical conductivity continue increasing sharply beyond 3.6 eV of photon energy as seen in Figure 8 suggesting strong excitation of the electrons. The volume energy loss function VELF and surface energy loss function SELF (volume and surface energy loss functions are proportional to the characteristic energy loss of fast electrons traveling the bulk and surface of the material, respectively) can be calculated using the following equations:

$$SELF = \frac{\varepsilon_2^2}{((\varepsilon_1+1)^2+\varepsilon_2^2)}$$

$$VELF = \frac{\varepsilon_2^2}{\varepsilon_1^2-\varepsilon_2^2}$$

The changes of VELF and SELF of as-prepared TiO_2 thin films with photon energy are shown in Figure 9; this change can be explained in terms of the response of a set of Lorentzian oscillators of adjustable strength and position (Ghanashyam et al., 1999). Wemple and DiDomenico (1973) introduced two parameters, the dispersion energy E_d which has a meaning of the

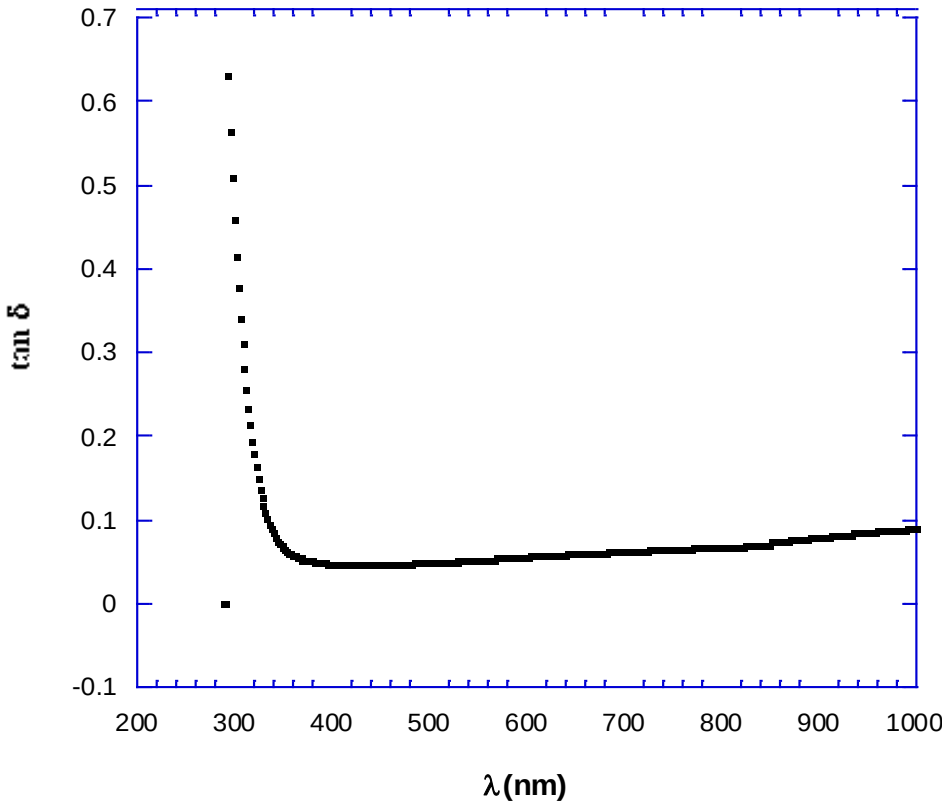

Figure 7. Variations of the loss factor δ with wavelength for TiO_2 thin films.

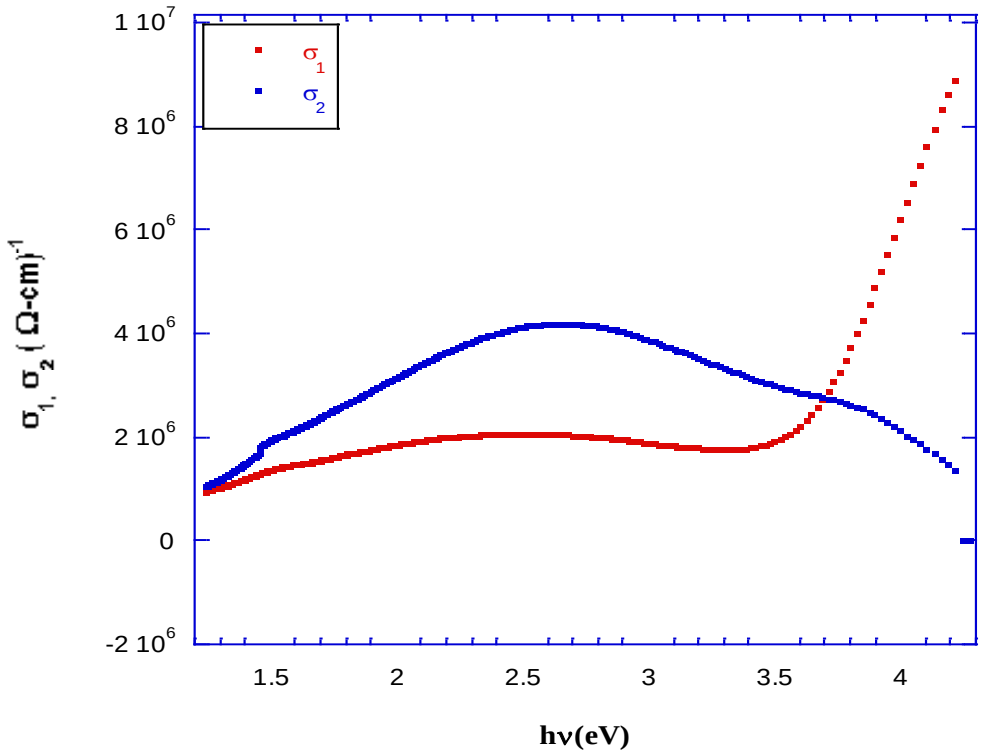

Figure 8. Spectra of the real and imaginary part of the optical conductivity of the TiO_2 thin films.

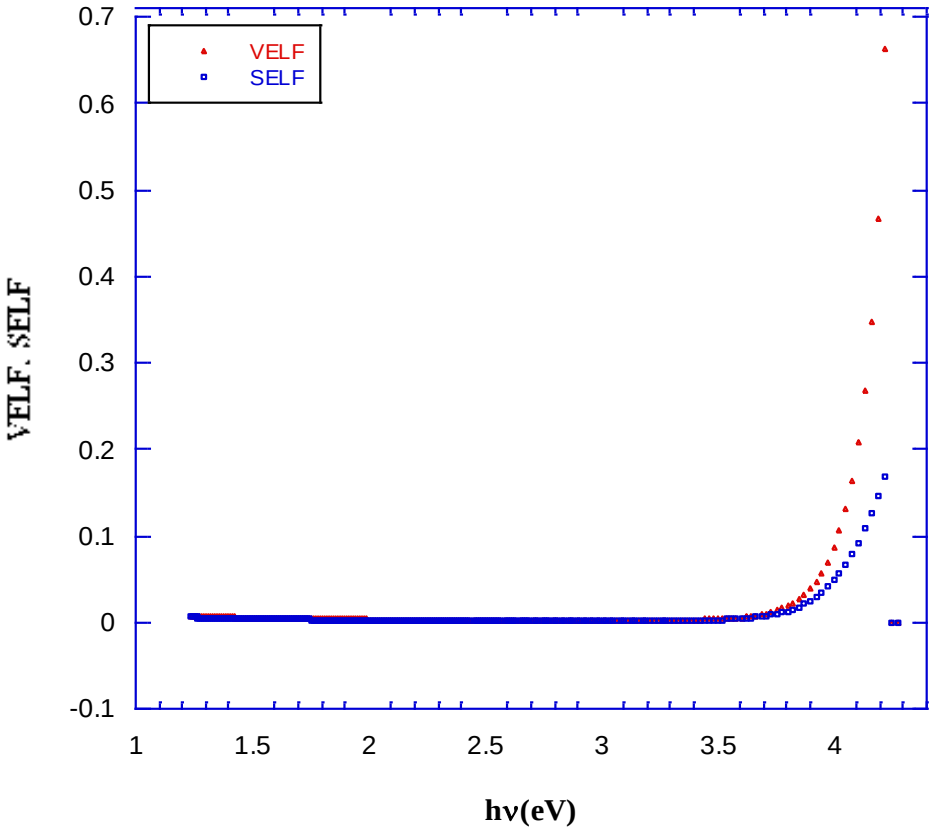

Figure 9. The distribution of the volume and surface energy loss for TiO_2 thin films as a function of thoton energy.

oscillator strength of the interband transition and describes the dispersion of the refractive index, and the single oscillator energy E_o which has a meaning of the average interband transition energy. Both of the two parameters can be calculated from the slope and intercept of Figure 10 and recorded in Table 1. The average value of the oscillator energy of the thin films under test is 3.486 eV which is in consistent to the optical energy gap estimated from Figure 3. This agree with Olomon et al. (1988) which reported that the single oscillator energy gives a quantitative information on the overall band structure of the material "average gap" and corresponds to the distance between the centers of gravity of the valence and conduction bands. The close value of the optical gap 3.36 eV and average value of single oscillator 3.486 eV is in good agreement with the relation reported by Timoumi et al. (2011). It is reported that the dispersion energy relates other physical parameters through the following empirical relationship (Wemple and DiDomenco, 1973; Timoumi et al., 2011):

$E_d = \beta N_c Z_a N_e$ (eV)

where N_c is the coordination number of the cation nearest – neighbor to the anion, Z_a is the formal chemical valency of the anion, N_e is the effective number of valence electrons per anion and β is a constant. Taking the experimental average value of E_d for the as deposited films (E_d=22.12 eV), Z_a = 2, N_c = 6, N_e = 6, then β = 0.31 eV, this leads to TiO_2 thin films under test fall into ionic class. The moments of the optical spectra M_{-1} and M_{-3} can be obtained from the relationship (Yakuphanoglu et al., 2004):

$$E_o^2 = \frac{M_{-1}}{M_{-3}} \quad , E_d^2 = \frac{M_{-1}^2}{M_{-3}}$$

It is found that the calculated values of the moments M_{-1} increase with increasing the thickness of the films, whereas the moments M_{-3} decrease. The ratio $(\frac{N}{m^*})$ and the lattice dielectric constant (the high frequency dielectric constant) ε_L for the thin films are calculated from Figure 11 which represents the plot of n^2 vs. λ^2 and then tabulated in Table 1. It can be noticed that both $(\frac{N}{m^*})$ and ε_L increases with increasing the thickness of the film from 100 to 150 nm.

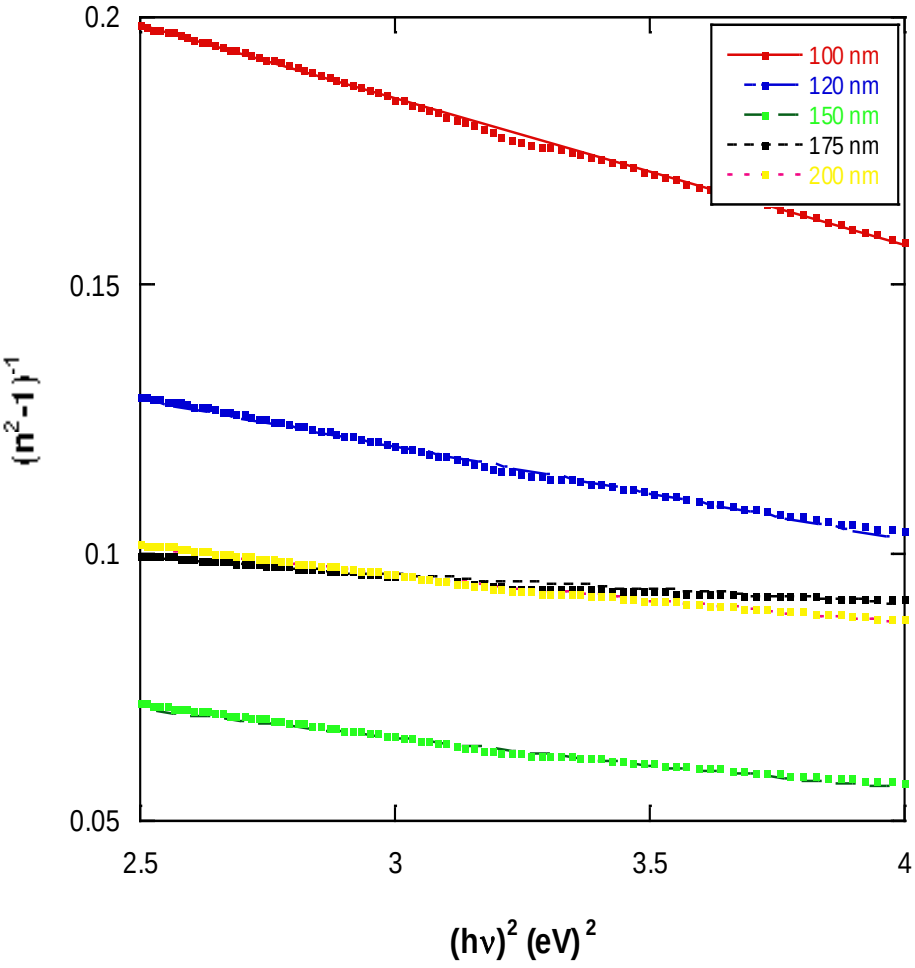

Figure 10. Plts of $(n^2 - 1)^{-1}$ vs. hν for as-prepared TiO_2 thin films of different thicknesses.

Table 1. The optical energy gap, Urbach energy, refractive index dispersion parameters of TiO_2 thin films.

Film thickness nm	E_g (eV)	E_u (eV)	E_o (eV)	E_d (eV)	β	M_{-1}	M_{-3} $(eV)^{-2}$	$(N/m^*)x10^{48}$ $(g^{-1}\ cm^{-3})$	ε_L
100	3.36	0.371	3.128	11.63	0.16	3.72	0.028	1.67	8.7
120	3.36	0.337	3.153	18.18	0.25	5.77	0.018	2.66	12.9
150	3.36	0.369	3.08	32.11	0.45	10.42	0.010	5.51	23.6
175	3.36	0.390	4.421	39.06	0.54	8.82	0.006	1.65	13.6
200	3.36	0.369	3.646	28.79	0.39	7.79	0.009	2.46	14.7

Conclusion

The optical properties of amorphous TiO_2 thin films under test showed that, changing the thickness of the films has not affected the optical energy gap and Urbach tails. The average value of the single oscillator energy has a value very close to that of the optical energy gap. The dispersion energy found to increase with increasing the thickness of the film, its average value used to estimate the value of β showing that TiO_2 under test is ionic. The moments M_{-1} showed an increase with thickness from 100 to 150 nm, whereas, the moments M_{-3} showed a decrease with thickness. Both $(\frac{N}{m^*})$ and ε_L showed an increase with thickness from 100 to 150 nm.

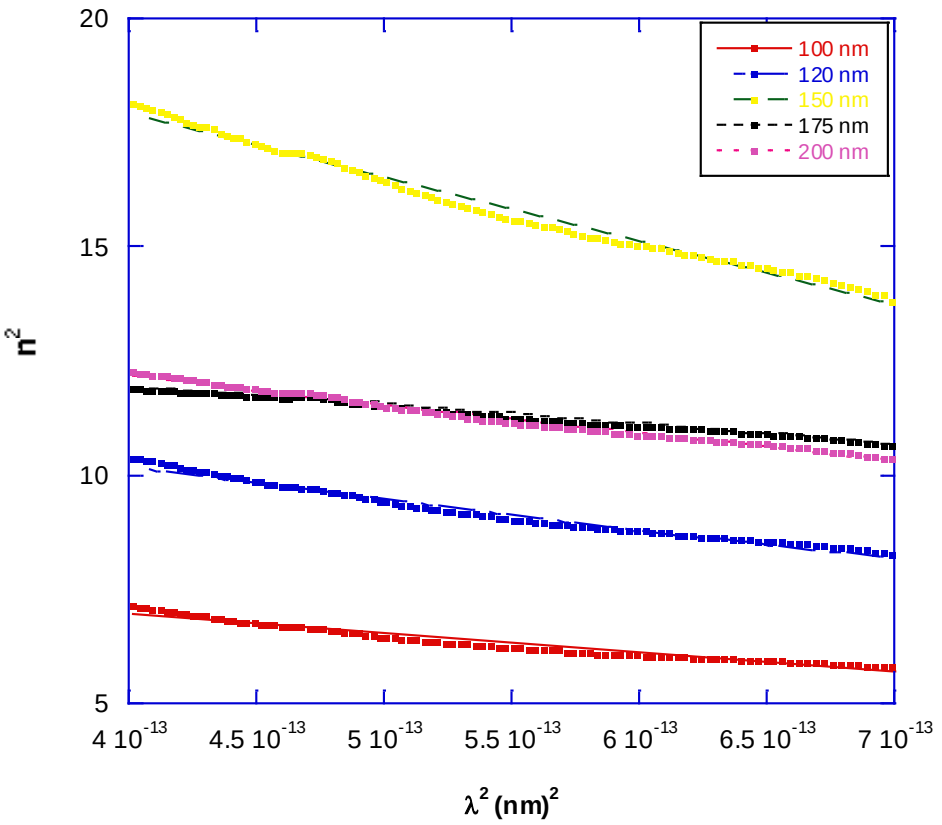

Figure 11. Plots of n^2 against λ^2 for as-prepared TiO_2 thin films of different thicknesses.

REFERENCES

Ali HM (2005). Characterization of a new transparent-conducting material of ZnO doped ITO thin films. Phys. Status Solidi A 202:2742-2752.

Al-Ofi' HH, Abd El-Raheem MM, Ateyyah M, Al-Baradi A, Atta A (2012). Structural And Optical Properties Of Al2zno4 Thin Films Deposited By Dc Sputtering Technique. J. Non-Oxide glasses 3:39-54.

Babuji B, Balasubramanian C, Radhakrishnan M (1983). Dielectric Properties Of Ion Plated Titanium Oxide Thin Films. J. Non-Crys. Solids 55:405-412.

Bakry AM, El-Naggar AH (2000). Doping Effects on the Optical Properties of Evaporated A-Si: H Films. Thin Solid Films pp. 360:293-297.

Bra¨uer G, Ruske M, Szczyrbowski J Teschner G, Zmelty A (1998) Mid frequency sputtering with TwinMag< sup>®-a survey of recent results, 51:655-659.

Caglar, Y, Ilican S, Caglar M (2007). Single-oscillator model and determination of optical constants of spray pyrolyzed amorphous SnO2 thin films. Eur. Phys. J. B 58-251-256.

Dislich H, Hinz P (1982). History and principles of the sol-gel process, and some new multicomponent oxide coatings. J. Non-Cryst. Solids 48:11-16.

Doeuff S, Henry M, Sanchez C, Symp MRS (1986). The Gel Route to Tio_2Photoanodes. 73:653.

Dumitriu D, Bally AR, Ballif C, Hones P, Schmid PE, Sanjinés R, Lévy F, Pârvulescu VI (2000). Photocatalytic degradation of phenol by TiO2 thin films prepared by sputtering, Appl. Catal. B. Environ. 25:83-92.

El-Nahass M (1992). Optical properties of tin diselenide films. J. Mater. Sci. 27:6597-6604.

El-Nahass M, Atta A, El-Sayed H, El-Zaidia E (2008). Structural and optical properties of thermal evaporated magnesium phthalocyanine (MgPc) thin films. Appl. Surf. Sci. 254:2458-2465.

El-Nahass M, El-Barry A, El-Shazly E, Omar H (2010). Structural and optical properties of thermally evaporated cadmium thiogallate CdGa2S4 nanostructure films. Eur. Phys. J. Appl. Phys. 52:10502..

El-Nahass M, Soliman H, Hendi D, Mady KA (1992). Effect of some growth parameters on vacuum-deposited CuInSe2 films. J. Mater. Sci. 27:1484-1490.

El-Raheem MA, Amry A, Al-Mokhtar M, Al-Jalali M, Amin S, El-Sayed H, Al-Ofi H (2012). Transport properties of Aluminum-Doped Zinc Oxide Thin Films. Adv. Mater. Corros. 1:30-35.

Ghanashyam Krishna M, Pillier JS, Bhattacharya AK (1999). Variable optical absorption edge in ion beam sputtered thin ytterbium oxide films. Thin Solid Films- 357:218-222.

Henry BM (1978). US Patent 4, 200.

Hou YO, Zhuang DM, Zhang G, Zhao M, Wu MS (2003). Influence of annealing temperature on the properties of titanium oxide thin film. Appl. Surface Sci. 218:98-106.

Livage J (1986). Synthesis, structure and applications of TiO2 gels, Cambridge Univ. Press, 73:717-724.

Lo¨ bl P, Huppertz M, Mergel D (1994). Nucleation and growth in TiO2 films prepared by sputtering and evaporation. Thin Solid Films 251:72-79.

Lottiaux M, Boulesteix C, Nihoul G, Varnier F, Flory F, Galindo R, Pelletier E (1989). Morphology and structure of TiO2 thin layersvs. thickness and substrate temperature. Thin Solid Films, 170:107-126.

Macleon HA (1986). Thin Film Optical Filters, 2^{ed} ed., Adam Hilger Ltd., Bristol, P. 71.

Nabavi N, Doeuff S, Sanchez C Livage J (1989). Sol-gel synthesis of electrochromic films. Mater. Sci. Eng. B. 3:203-207.

Ozer N, Tepehan F, Bozkurt N (1992). An "all-gel" electrochromic

device. Thin Solid Films 219:193-198.
Pal U, Samanta D, Ghori S, Chaudhuri AK (1993). Optical constants of vacuum-evaporated polycrystalline cadmium selenide thin films. J. Appl. Phys. 74(10):6368-6374.
Pulker HK (1984). Coatings on Glass. Elsevier Science Publishers B. V. P. 311.
Ritter E (1975). Dielectric film materials for optical applications. Phys. Thin Films 8:1.
Robert M Jr., Morel DL, Ferekides CS (2005). Transparent conducting oxide thin films of Cd2SnO4 prepared by RF magnetron co-sputtering of the constituent binary oxides. Thin Solid Films 484:26-33.
Solomon I, Schmidt MP, Senemaud C, Khodja MD (1988). Band structure of carbonated amorphous silicon studied by optical, photoelectron, and x-ray spectroscopy. Phys. Rev. B 38:13263.
Takeda S, Suzuki S, Odaka H, Hosono H (2001). Photocatalytic TiO2 thin film deposited onto glass by DC magnetron sputtering. Thin Solid Films 392:338-344.
Takeda, S, Suzuki S, Odaka H (2001). Photocatalytic TiO2 thin film deposited onto glass by DC magnetron sputtering. Thin Solid Films. 392(2):338-344.
Timoumi A, Bouzouita H, Rezig B (2011). Optical constants of Na-In2S3 thin films prepared by vacuum thermal evaporation technique. Thin Solid Films 519:7615-7619.
Treichel O Kirchhoff V (2000). The influence of pulsed magnetron sputtering on topography and crystallinity of TiO2 films on glass. Surf. Coat. Technol. 123:268-272.
Urbach F (1953). The long-wavelength edge of photographic sensitivity and of the electronic absorption of solids. Phys. Rev. 92:1324.
WatanabeT, Fukayama S, Miyauchi M, Fujishima A, Hashimoto K (2000). Photocatalytic activity and photo-induced wettability conversion of TiO2 thin film prepared by sol-gel process on a soda-lime glass. J. Sol–Gel Sci. Technol. 19:71-76.
Wemple SH (1973). Refractive-index behavior of amorphous semiconductors and glasses. Rev. B. 7:3767.
Wemple SH, Didomenico Jr M (1971). Behavior of the electronic dielectric constant in covalent and ionic materials. Phys. Rev. B. 3:1338.
Yakuphanoglu F, Cukurovali A, Yilmaz I (2004). Determination and analysis of the dispersive optical constants of some organic thin films. Phys.B: Condensed Matt. 351:53-58.
Ya-Qi H, Da-Ming Z, Gong Z, Ming Z, Min-Sheng W (2003). Influence of annealing temperature on the properties of titanium oxide thin film. Appl. Surf. Sci. 218:97.
Yeung KS Lam YW (1983). A simple chemical vapour deposition method for depositing thin TiO2 films. Thin Solid ilms, pp. 109:169-178.
Yoko T, Kamiya K, Yuasa A, Tanaka K, Sakka S (1988). Surface modification of a TiO2 film electrode prepared by the sol-gel method and its effect on photoelectrochemical behavior. J. Non-Cryst. Solids 100:483-489.
Yoldas BE (1980). Investigations of porous oxides as an antireflective coating for glass surfaces. Appl. Opt. 19:1425-1429.
Yun, H, Miyazawa K, Honma I, Zhou H, Kuwabara M (2003). Synthesis of semicrystallizedmesoporous TiO2 thin films using triblock copolymer templates. Mater. Sci. Eng. C. 23:487-494.
Zhang F, Huang, N, Yang P, Zeng X, Mao Y, Zheng Z, Zhou Z, Liu X (1996). Blood compatibility of titanium oxide prepared by ion-beam-enhanced deposition. Surf. Coat. Technol. 84:476-479.